ARTICLE

Hazard Assessment and Hazard Mapping for Kuwait

Ali Al-Hemoud[1] · Abdulla Al-Enezi[1] · Hassan Al-Dashti[2] · Peter Petrov[1] · Raafat Misak[3] · Manar AlSaraf[1] · Mariam Malek[1]

Abstract

Hazard maps are essential tools to aid decision makers in land-use planning, sustainable infrastructure development, and emergency preparedness. Despite the availability of historical data, there has been no attempt to produce hazard maps for Kuwait. In cooperation with the World Bank, this study investigated the natural and anthropogenic hazards that affect Kuwait. The objective was to assess the hazards that face Kuwait and map the hazards of most concern. Hazard maps depicting the spatial distribution of hazard-prone areas are discussed in this article. Hazard assessment maps were generated using multiple datasets and techniques, including meteorological data, satellite imagery, and GIS. Hazard profiling identified a total of 25 hazards, of which five "priority" hazards were explored in detail: (1) surface water flooding; (2) dust storms and sand encroachment; (3) drought; (4) air pollution; and (5) oil spills. The results of this study can aid decision makers in targeting the hazards of most concern. The developed maps are valuable tools for emergency response and hazard mitigation.

Keywords Hazard mapping · Hazard prioritization · Hazard profiling · Kuwait

1 Introduction

Hazards are processes, phenomena, or human activities that may cause loss of lives, injuries or other health impacts, property damages, social and economic disruptions, or environmental degradation (UNDRR 2022). Hazards may be natural (associated with natural processes or phenomena, for example, earthquakes), anthropogenic (human-induced hazards, for example, air pollution), or socionatural in origin (associated with a combination of natural and anthropogenic factors, including environmental degradation and climate change). Disasters are serious disruptions to a community's functioning or society at any scale due to hazardous events. These definitions align with the United Nations Office for Disaster Risk Reduction (UNDRR 2022). Hazardous events may occur simultaneously, cascadingly, or cumulatively over time, considering the potential interrelated effects (Tilloy et al. 2019; UNDRR 2022). Earthquakes may lead to landslides (Miles and Keefer 2009; Bathrellos et al. 2017; Pourghasemi et al. 2019), floods and landslides are triggered by extreme rainfall (Liu et al. 2018; Nachappa et al. 2020), and dust storms may lead to sand encroachment (Al-Hemoud et al. 2019). It is essential to classify the country's hazards and prioritize the hazards of most concern. In addition to the hazard aspect, risk is a function of hazard, exposure, vulnerability, and capacity (Park et al. 2020). In this article, we present only the hazard assessment and mapping concept without reference to vulnerability assessment/mapping or risk assessment/mapping.

Worldwide, humans are faced with high risks from natural and anthropogenic hazards. Climate change will lead to increased risks and intensity of natural hazards, particularly droughts, heavy rains, and river floods (Athimon and Maanan 2018). Rising sea levels due to global warming can result in losses to coastal communities' infrastructures (Sajjad et al. 2018; Allen et al. 2019). Threats posed by climate change can lead to floods (Shah et al. 2018; Song et al. 2019) and droughts (Dabanli 2018; Orimoloye et al. 2021). Floods have been shown to affect large communities in East Africa (Kalantari et al. 2018), the Indian subcontinent (Asim et al. 2019), and Australia (Rolfe et al. 2020). Many countries,

✉ Ali Al-Hemoud
ahomood@kisr.edu.kw

1 Crisis Decision Support Program, Environment and Life Sciences Research Center, Kuwait Institute for Scientific Research (KISR), Safat, 13109 Kuwait City, Kuwait

2 Meteorology Department, Directorate General of Civil Aviation, 32001 Hawalli, Kuwait

3 Desert Research Center, Cairo, Egypt

other than those located in the arid and semiarid regions, are affected by droughts—for example, South Korea (Nam et al. 2015; Bae et al. 2018; Mun et al. 2020), Western Europe, and northern Scandinavia (Spinoni et al. 2018). Besides floods and droughts, dust storms can heavily affect communities. Asian dust has been shown to affect large communities in Japan (Michikawa et al. 2020), while Sahara dust has been shown to affect parts of the Caribbean, Central America, and the United States (Urrutia-Pereira et al. 2021).

Kuwait has been particularly affected by sand and dust storms (SDSs). Recurrent SDS events result in oil export losses due to the closure of marine terminals, airline delays due to airport shutdowns, agricultural land degradation, human health disorders, and solar power productivity losses (Li et al. 2020). Due to intensive SDS events, sand encroachments result in roadblocks and traffic accidents. Kuwait is also vulnerable to surface water flooding, extreme temperatures, drought, air pollution (Al-Hemoud, Al-Khayat et al. 2021; Alahmad et al. 2021), and marine oil spills (Park et al. 2019).

The development of disaster risk profiles is essential for any country to reduce existing disaster risks, prevent new risks, and manage residual risks, all of which contribute to strengthening resilience and capacities (Bang 2022). With knowledge of the prevailing hazards, population vulnerability, and socioeconomic development, risk can be assessed and mapped (UNDRR 2022). Kuwait lacks risk zoning, and only rudimentary hazard assessments exist due to limited comprehension and profiling of risk.

Hazard mapping can highlight areas affected by a particular hazard, for example, air pollution (Park et al. 2020). Two steps are required for hazard mapping. The first involves selecting the study area and identifying all potential hazards, and the second requires the use of geospatial techniques for hazard mapping. In the first step, historical and existing hazard data are collected, including base maps and hazard maps. It also involves collecting country profile data (for example, from the population and housing census). In the second step, geospatial techniques such as remote sensing and geographic information systems (GIS) are common tools for hazard mapping (Nyarko et al. 2015; Ntajal et al. 2017; Tahmid et al. 2020; Tomaszewski et al. 2020). Hazard data acquisition and dissemination require cooperation and commitment from government agencies and local partners because such data are unavailable in only one sector. Questionnaires are well-established tools for acquiring information on hazards (Bird 2009). Questionnaires have been used to collect data for hazard projects, including earthquakes (Lindell and Whitney 2000), floods (Brilly and Polic 2005; Sarmah et al. 2020), landslides (Solana and Kilburn 2003), cyclones (Anderson-Berry 2003), and volcanic eruptions (Haynes et al. 2008; Clive et al. 2021). Focus groups and face-to-face interviews can generate insightful and valid data

and provide directions for clarifying questions and participation. To our knowledge, hazard assessment and mapping have not been carried out in Kuwait. This study aimed to assess the hazards that face Kuwait and map the hazards of highest priority.

2 Method

This section describes the approach followed for hazard data collection and analysis. It presents the approach to assess and prioritize hazards in Kuwait.

2.1 Study Area

Kuwait's total area is approximately 18,000 km^2 and the country lies between latitudes 28.45°N and 30.05°N, and longitudes 46.30°E and 48.30°E. It is located in the Arabian Peninsula, at the northern edge of the Arabian/Persian Gulf, bordering Iraq to the north and Saudi Arabia to the south, and has approximately 300 km of coastline to the east. Kuwait's total population is around five million, and almost all of the country's population lives in urban areas, about 7% of the country, and the remaining area (93%) is considered desert. Kuwait registered the highest temperature ever recorded in Asia at 54 °C (129 °F) at Mitribah on 21 July 2016 (Merlone et al. 2019). High summer temperatures often exceed 45 °C, and low nighttime winter temperatures frequently drop below 8°C. Urban cool islands dominate during the day, while urban heat islands dominate at night, during the day, the temperature difference (urban versus rural) is − 1.1 °C, while at night, the temperature difference is 3.6 °C (Alahmad et al. 2020). The Shamal, a north-westerly wind, is common during the summer and causes intensive dust storms, particularly in June and July (Yassin et al. 2018). Annual rainfall is slightly higher than 100 mm, and occurs mainly from November to April in the form of showers. Although rainfall is scarce, torrential rain can cause surface water flooding with devastating impacts.

2.2 Hazard Profiling

There is no standardized approach to assessing hazards. The qualitative approach through hazard classification is the most widely used approach to characterize and compare hazards (Kappes et al. 2012). Properly designed questionnaires and workshops are appropriate for hazard data collection (Chouhan and Mukherjee 2022). Applying scaling and weighting methods, along with questionnaires and surveys, are commonly used to assess hazards (Pandey and Jha 2012; Yadav and Barve 2017; Ahmed and Kelman 2018).

As feedback from stakeholders influences the interpretation of hazard identification and prioritization, a 4 day

hazard profiling workshop was conducted in Kuwait with the cooperation of the World Bank (26–29 March 2018). The objectives of the workshop were twofold: (1) to scope out the availability of hazard data and hazard maps from the various local authorities in Kuwait; and (2) to prioritize the hazards of most concern in Kuwait. Hazard data (for example, historic drought) were requested from various governmental/institutional stakeholders (for example, the Kuwait Meteorological Department, the Kuwait City Municipality), including base maps (for example, land use, coastal zonation, topography, bathymetry, and soil typology maps) and hazard-related maps (for example, seismic activity and floodplain maps). Country profile data (for example, population, settlement, housing census, socioeconomic, educational, health, and infrastructure sectors such as airports, industries, power stations, roads) were also requested. The workshop served as the baseline for data collection and provided a detailed understanding of the potential hazards that affect Kuwait.

The outcome of the workshop was the development of a questionnaire. The questionnaire was critical for this study and served as the hazard data collection and mapping baseline. The questionnaire was distributed to the participating stakeholders to collect hazard information. A second 4 day workshop (23–26 April 2018) with the World Bank and the stakeholders was conducted one month later in Kuwait. A total of 23 participants from 10 governmental/institutional stakeholders participated in each workshop. Ten questionnaires were distributed to the participating stakeholders and all 10 questionnaires were returned (one questionnaire for each governmental/institutional stakeholder). The purpose of the second workshop was twofold: (1) to collect the filled-out questionnaires; and (2) to discuss the hazards that face Kuwait and to prioritize the hazards of most concern. The questionnaire included nine sections that requested:

(1) Data on hazards, exposures, vulnerabilities, and risk assessments;
(2) Data and maps for carrying out hazard assessments;
(3) Data and maps for understanding the exposure of the population and economic sectors;
(4) Information on hazard and exposure data quality;
(5) Information on existing vulnerability and risk data;
(6) Information on risk governance mandates;
(7) Information on financing mechanisms for investing in risk management;
(8) Information on mechanisms for multidisciplinary coordination; and
(9) Information on the degree to which national investment and development strategies are risk sensitive (a copy of the questionnaire is available on request).

To prioritize the hazards that face Kuwait, four types of information were collected: (1) the total number of recorded hazards; (2) the manifestation of the hazards in terms of low, moderate, or high hazardous events; (3) the hazard impact to the economy in terms of monetary losses, lives lost, and primary service losses (for example, power outages); and (4) community resilience. Hazard assessment was agreed upon between the World Bank and the 10 governmental/institutional stakeholders using a combination of theory-driven, data-driven, and normative approaches (Nguyen et al. 2016). The theory-driven (deductive) approach is based on existing scientific knowledge to identify the hazards and their relationships (Mahendra et al. 2011); the data-driven (inductive) approach is based on the statistical relationship between the hazards and their outcomes (for example, mortality due to earthquakes) (Eriksen and Kelly 2007); and the normative approach is based on the collective expert opinion (for example, the Delphi method) (Kienberger et al. 2009).

2.3 Hazard Prioritization

A total of 25 hazards were shown to affect Kuwait (Table 1). These hazards were considered in terms of their potential interrelated effects. Kuwait has long historical records for many hazards (for example, 1962–2018; 57 years). The authors prepared hazard summaries detailing hazards and their impacts specific to Kuwait. The hazard summaries essentially include four types of information: (1) a catalogue of historical disasters and their impacts and data sources; (2) a hazard summary of Kuwait; (3) a hazard summary with a focus on the city of Kuwait; and (4) a refined approach towards the assessment of hazards individually and in a multi-hazard context (for future studies). The authors carried out desk reviews, created hazard-wise summaries, and cataloged historical disasters at the national and Kuwait City levels. The recorded hazard events ranged from 6 (sinkholes) to 1482 (explosive remnants of war). The macro-hazard assessment covering these hazards was performed based on available data (where data were not locally available, the project consultant risk management solutions, Inc. (RMSI) filled the data gaps using global datasets).

A total of nine hazards were considered significant (high hazard manifestation, high hazard impact, and low societal coping capacity): (1) surface water flooding; (2) dust storms and sand encroachment; (3) drought; (4) air pollution; (5) oil spills; (6) fish kills; (7) waterlogging; (8) seawater temperature; and (9) landfill fires.

Five hazards were identified as "high priority" by consensus of the governmental/institutional stakeholders: (1) surface water flooding; (2) dust storms and sand encroachment; (3) drought; (4) air pollution; and (5) oil spills.

Table 1 Primary data for preliminary hazard assessment and hazard prioritization for Kuwait (arranged by year) ("high priority" hazards are marked in bold)

Hazard	Year	No. of events	Hazard manifestation (No. of low/moderate/high)	Impact on economy (USD Million)	Impact on lives (dead/injured/sick/displaced/affected)	Impact on basic services (Ex. days of interruption)	Resilience
1. Industrial accidents	2000, 2006, 2011, 2018	27	16/6/5	10	10/50/100/230		High
2. Fish kills, harmful algae, bleaching	1999−2018	16	2/2/12				Low
3. Earthquakes	1998−2018	1047	1038/9/0				Medium
4. Landfill fires	1998−2018	10					Low
5. Waterlogging and salinization	1997−2018	160					Low
6. Air pollution	1990−2018	7	3/3/1		1/14/na/na/na		Low
7. Seawater pollution	1990−2018	15	2/5/8			6 months	Medium
8. Animal diseases	1990−2018	19	14/1/4		392/2/na/45		High
9a. Oil spills	1990−2018	12	8/3/1		na/6/na/na/na		Low
b. Oil spills— Gulf War (1990)	1990	301	0/0/301				High
10. Explosive remnants of war	1990−2018	1482	0/1,246/236				High
11. Sinkholes	1988−1989	6	4/1/1				High
12. Seawater temperature	1985−2018						Low
13. Water-table rise in residential areas	1981−1983						Medium
14a. Dust storms	1962−2018	862		Annual 156			Low
b. Sand encroachment	1962−2018	859	213/213/426	Annual 2			Low
15. Surface water flooding	1962−2018	15	7/4/4		11/na/na/na/na		Low
16. Drought	1962−2018	7	3/1/3				Low

17−25 Other hazards with no data–17. Tsunamis; 18. Landslides; 19. Storm surges; 20. Food insecurity; 21. Groundwater depletion; 22. Eutrophication; 23. Rising sea levels; 24. Radiation exposure; 25. Infrastructure network failure (water and electricity).

3 Results

This section analyzes the five "priority" hazards and provides hazard mappings for: (1) surface water flooding; (2) dust storms and sand encroachment; (3) drought; (4) air pollution; and (5) oil spills.

3.1 Surface Water Flooding

Surface water flooding is primarily a result of high-intensity rainfall events. Surface water flooding frequently occurs in Kuwait because of poor water runoff design and sewage discharge. Surface water flooding—generally associated with heavy rainfall events over short periods of time—has caused large-scale damages in terms of the impact on lives and the economy. For instance, 27 mm of rainfall occurred in just one hour on 14 November 2018 in Al-Taweel district, south of Kuwait City. It caused severe flooding, killing one person and damaging around USD 328 million worth of property (Newarab 2018).

There is no standardized nomenclature, or agreed practices, for flood hazard mapping (Nones 2017). The first step in the quantitative surface water flood assessment was to understand the characteristics of the flood-producing rainfall events. A meteorological analysis was undertaken to estimate the rainfall volume, varying from the most frequent to rare. A frequency analysis of historical rainfall was carried out to determine the rainfall intensities for a range of return periods. Rainfall analysis was carried out using the available hourly and daily rainfall data. The analysis used
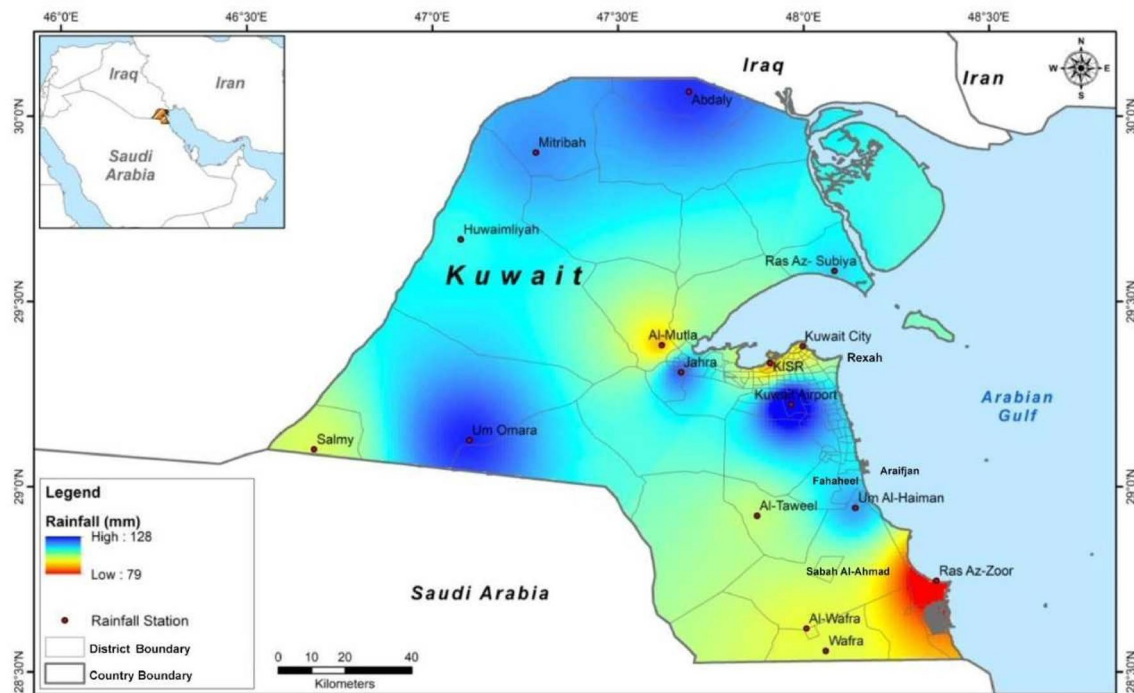
Fig. 1 Spatial distribution of average annual rainfall in Kuwait, 2013–2018. *Source* Kuwait Institute for Scientific Research (KISR)

16 rainfall stations comprising daily and hourly rainfall values. Figure 1 shows the spatial variation of average annual rainfall in Kuwait for six years (2013–2018). Out of the 16 stations, the Kuwait airport station recorded the maximum yearly average rainfall of about 128 mm, while Ras Az-Zoor station recorded the lowest at 79 mm.

Basin delineation was carried out using the United States Army Corps of Engineers (USACE) Hydrologic Engineering Center hydrologic modeling system (HEC-HMS). The hydrologic model helps identify water runoff discharge by simulated rainfall-runoff processes (Hamdan et al. 2021). The hydrological model was used utilizing the Geospatial hydrologic modeling extension (HEC-GeoHMS) and Arc-GIS. For basin delineation of the study area, the digital elevation model (DEM)/digital terrain model (DTM) (ASTER 30 m) was used. The unsteady 2D HEC-RAS model simulation was started after setting up parameters like flow parameters and upstream/downstream boundary conditions. A total of 40 basins were delineated, of which 30 were small with areas of less than 100 km^2, and the remaining 10 basins were large, with areas ranging from 142 to 10,270 km^2 (Fig. 2).

A 2D hydraulic model developed by the HEC river analysis system was used to predict the floodplain inundation. The primary purpose of hydraulic modeling is to route the flows from one location to another while estimating the water surface elevations and profiles for various scenarios (Grimaldi et al. 2013). Generally, the flows or water surface elevations observed at a particular location are given as inputs to the model, along with channel characteristics, such as cross-section, slope, and roughness (Lamichhane and Sharma 2018). The upstream boundary condition was provided as a return period flow hydrograph at the upstream section. The outlet boundary was given in terms of downstream boundary conditions in the form of average depth. A set of simulation parameters like simulation time, time step, mapping output interval, and detailed output intervals were given while running the model for any return period event. The typical output from the model was evaluated for floodwater depth. The computational 2D mesh for the floodplain area was generated using the geometric editor of HEC-RAS with a nominal grid resolution (50 m × 50 m cell size) for the Kuwait study area.

Hazard mapping for surface water flooding for the Kuwait basins was simulated using the 2D HEC-RAS models and ArcGIS (Fig. 3). A flood hazard mapping shows the spatial extent and depth of flooding at specific water-level intervals and has been featured in many studies using HEC-RAS and GIS (Mokhtar et al. 2018; Sathya and Thampi 2021; Tamiru and Dinka 2021).

A simulation of the flood model was prepared using the hourly rainfall data of 4–14 November 2018, a significant flood event. A flood depth in the range of 0.5 to 0.7 m was computed for two heavily impacted cities, Sabah Al-Ahmad and Fahaheel. The flood hazard map shows that
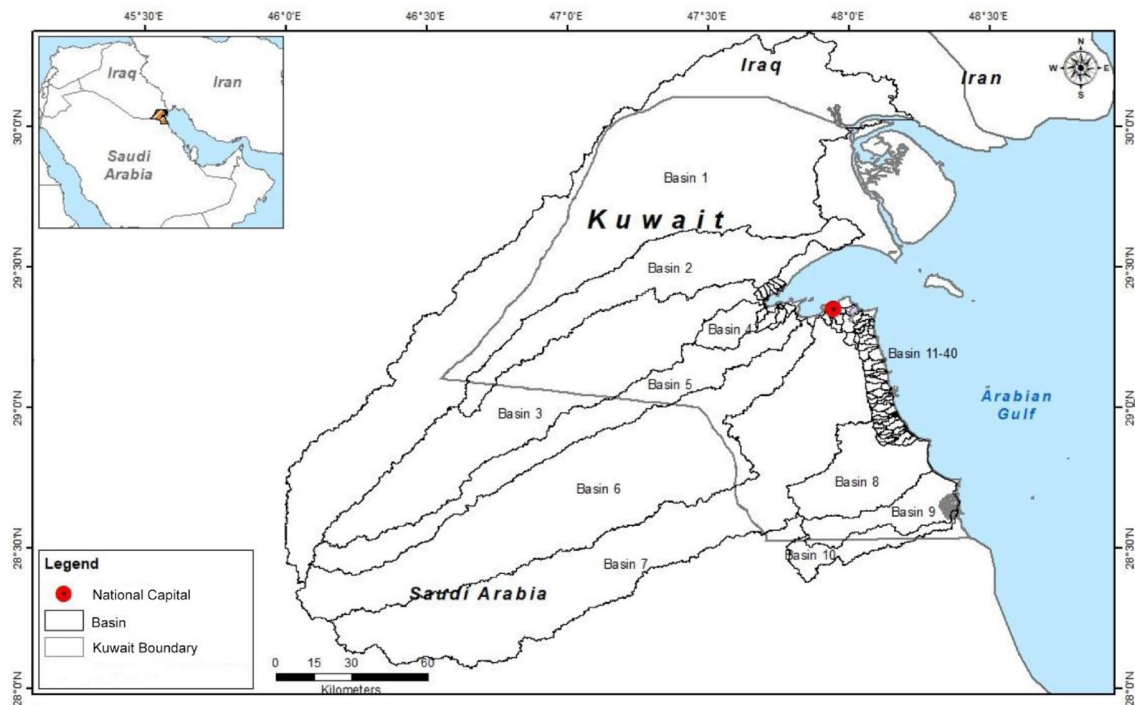
Fig. 2 Spatial distribution of the 40 water-runoff (river) basins in Kuwait. *Source* Kuwait Institute for Scientific Research (KISR)
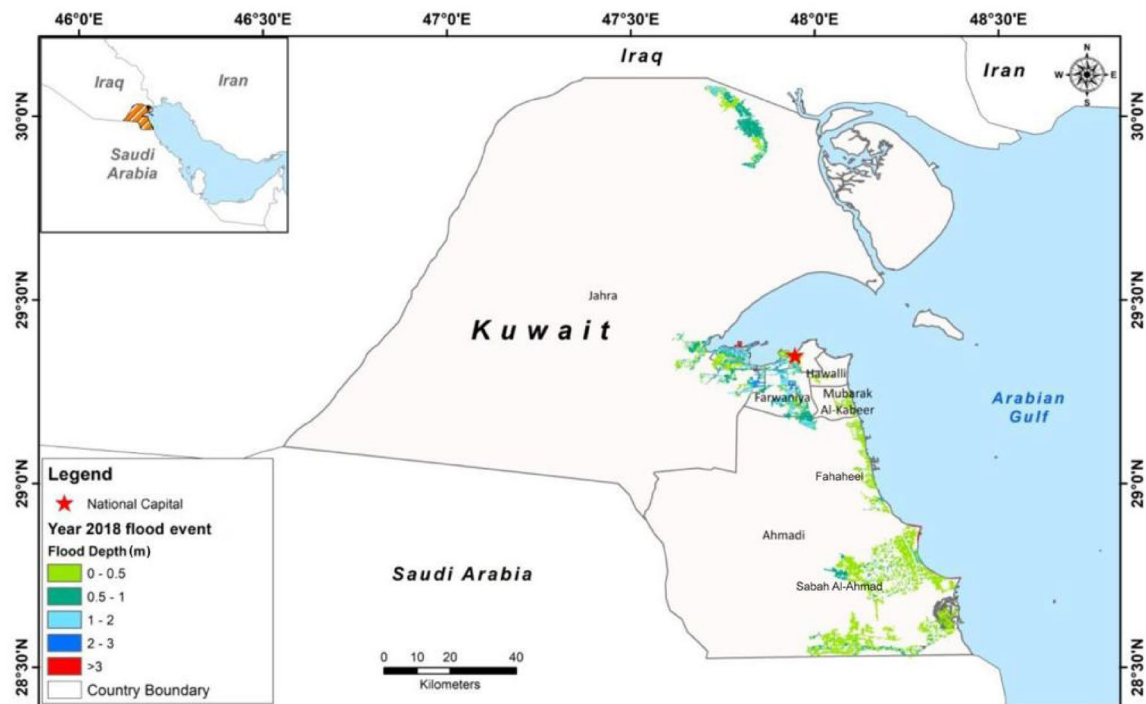

Fig. 3 Flood hazard map for Kuwait based on a major flood event, 4–14 November 2018. *Source* Kuwait Institute for Scientific Research (KISR)

Kuwait City, the coastal area, north (Abdaly), and south (Sabah Al-Ahmad and Wafra) are highly affected by floods.

Similar studies used GIS-based hazard mapping to identify flood-prone areas (Feng et al. 2020; Antzoulatos et al. 2022).
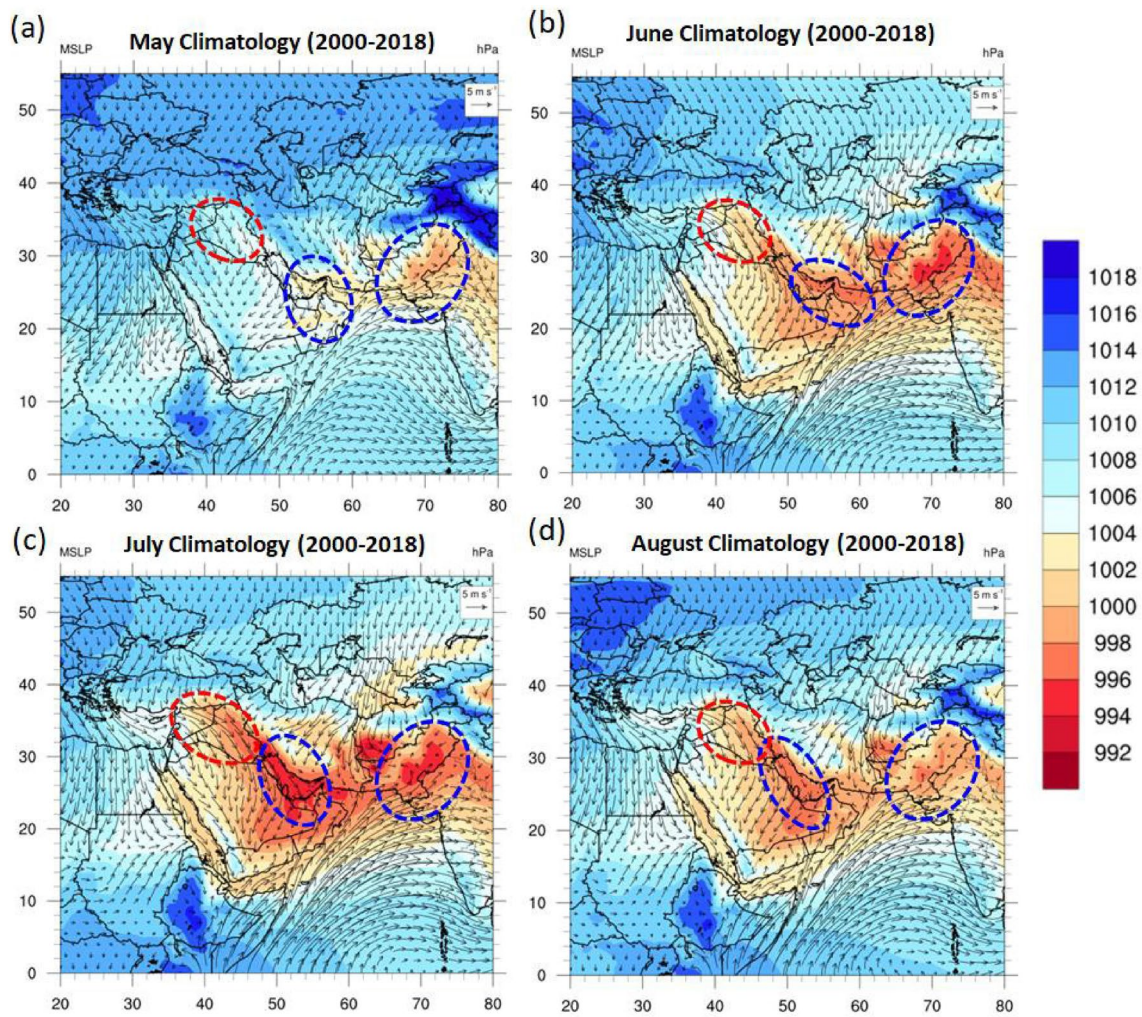
Fig. 4 Mean sea level pressure (MSLP) (hpa) and wind field maps over the Middle East and Southwest Asia extracted from ERA-Interim reanalysis, 2000–2018: **a** May; **b** June; **c** July; **d** August

3.2 Dust Storms and Sand Encroachment

Large-scale synoptic weather systems have primary control over the episodic and seasonal dust storm events over most dust source regions, including Kuwait. A sufficiently large low-level pressure gradient drives strong winds capable of dust emission and long-range transport (Hermida et al. 2018). The heat lows over the Arabian Peninsula (AP) start in May, rising to their peak in July, then gradually slow down by October (Francis et al. 2021). From 2000 to 2018, the ERA-Interim monthly mean analysis showed that the most prominent heat lows over the AP were observed during June, July, and August (Fig. 4). During these summer months, there were two main continental heat lows. The first (low-pressure area) was established over the border of India and Pakistan (right blue dashed line circles), and the second was established over the AP (middle blue dashed line circles). The

areas with strong inflow into the AP heat lows are marked with red dashed circles located northwest of Kuwait. The strong airstreams pass over the dust source region leading towards the marked heat lows bringing more frequent dust storms over Kuwait and adjacent areas during June, July, and August compared to the rest of the months.

Five major dust source regions that affect Kuwait were identified, including the western desert of Iraq, the Mesopotamian floodplain in Iraq, the northern desert of Saudi Arabia, the drained marshes in southern Iraq, and the dry marshes and abandoned farms in southwest Iran (Al-Dousari and Al-Awadhi 2012). Kuwait is highly prone to dust storm trajectories from the middle Euphrates region, specifically from two "hot spot" areas in the Mesopotamian floodplain (Al-Hemoud et al. 2020).

Dust load hazard mapping over the AP and Kuwait was simulated using the WRF-Chem model. The accuracy of the WRF-Chem model was validated using the moderate
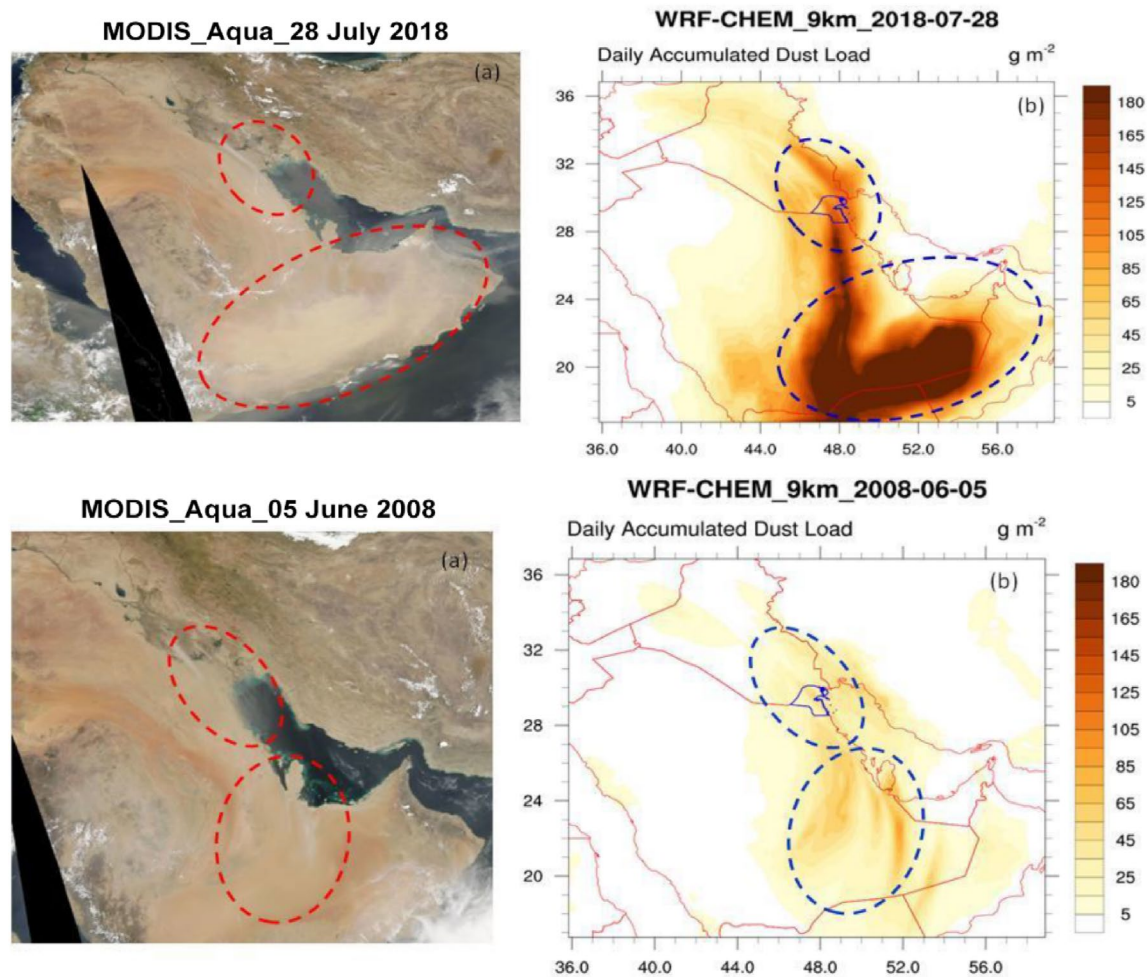
Fig. 5 Dust load hazard map for Kuwait based on **a** a strong dust storm on 28 July 2018; and **b** a moderate dust storm on 5 June 2008. *Source* Kuwait Institute for Scientific Research (KISR)

resolution imaging spectroradiometer (MODIS) Aqua satellite images for two dust storm events—a moderate one on 5 June 2008, and a strong one on 28 July 2018 (Fig. 5). The WRF-Chem model was in good agreement with the satellite image processed by MODIS. The model delineated the total dust load over central and southern Saudi Arabia but underestimated the dust load over Kuwait—previous studies have shown similar results (Al-Hemoud et al. 2020).

Sand encroachment hazard mapping using ArcGIS is a common tool to identify hot spot sand sources (Gómez et al. 2018; Mehrabi 2020; Abdullah et al. 2021). Generally, there are seven sand encroachment hazard drivers: sand drift potential/wind energy; surface sediment; vegetation density; land use; drainage density; topographic change; and vegetation type. A raster calculator, a spatial analyst function in ArcGIS, was used to delineate sand encroachment. A sand encroachment hazard map was created (Fig. 6). Zones of very high and high sand encroachment cover approximately 35% (6060 km^2) and 22% (3841 km^2) of the total area of

Kuwait, respectively. Out of 159 districts, very high sand encroachment stretches from Al-Mutla and south of Rexah in the mid-west toward Araifjan and Al-Wafra in the southwest. High sand encroachment is mostly located in the west and south of Kuwait, including some scattered zones in the north and northwest.

3.3 Drought

Drought is a severe hazard in Kuwait and the neighboring countries (Nasrollahi et al. 2018). During the last four decades, Kuwait experienced two dry periods with annual average rainfall below 110 mm (1982–1992 and 2006–2017). Drought results in soil loss and dust emission, natural vegetation dryness, soil moisture depletion, and biodiversity loss (Cook et al. 2018; Chiang et al. 2021; Orimoloye et al. 2021). In a freshwater-scarce country like Kuwait, the impact of drought cannot be overstated.
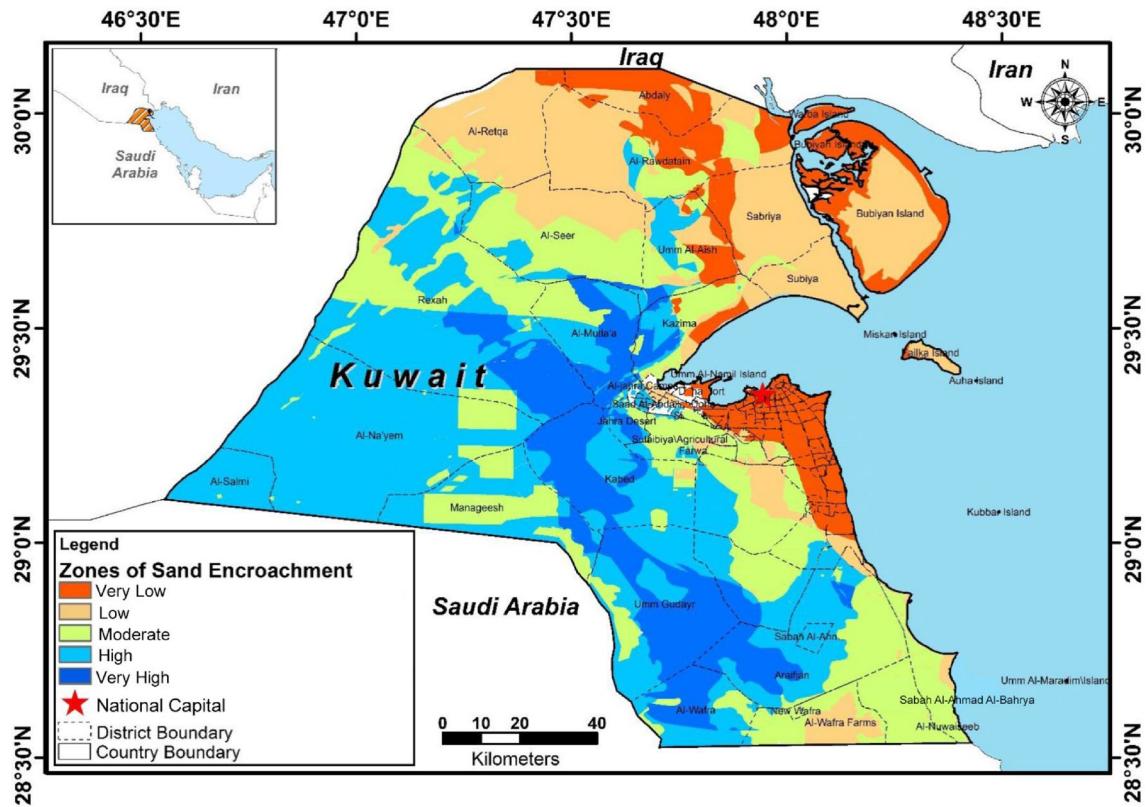
Fig. 6 Sand encroachment hazard map for Kuwait. *Source* Kuwait Institute for Scientific Research (KISR)
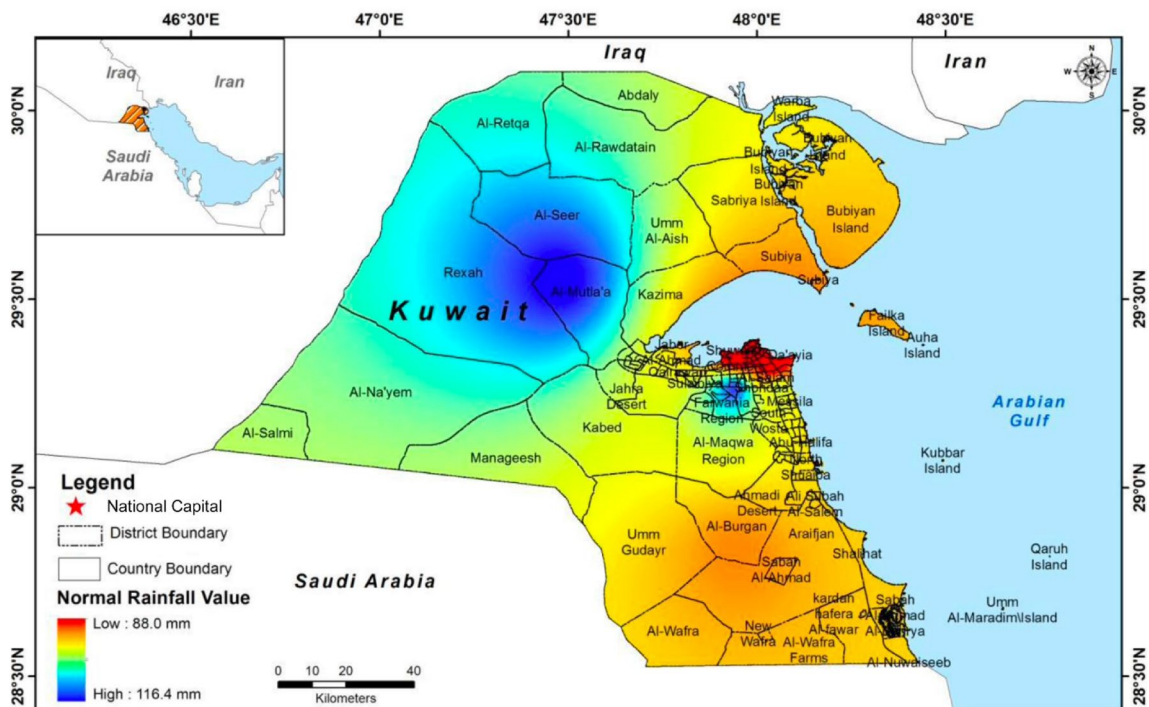

Fig. 7 Average annual rainfall spatial distribution map for the rainy season (October–May) in Kuwait, 1981–2018. *Source* Kuwait Institute for Scientific Research (KISR)
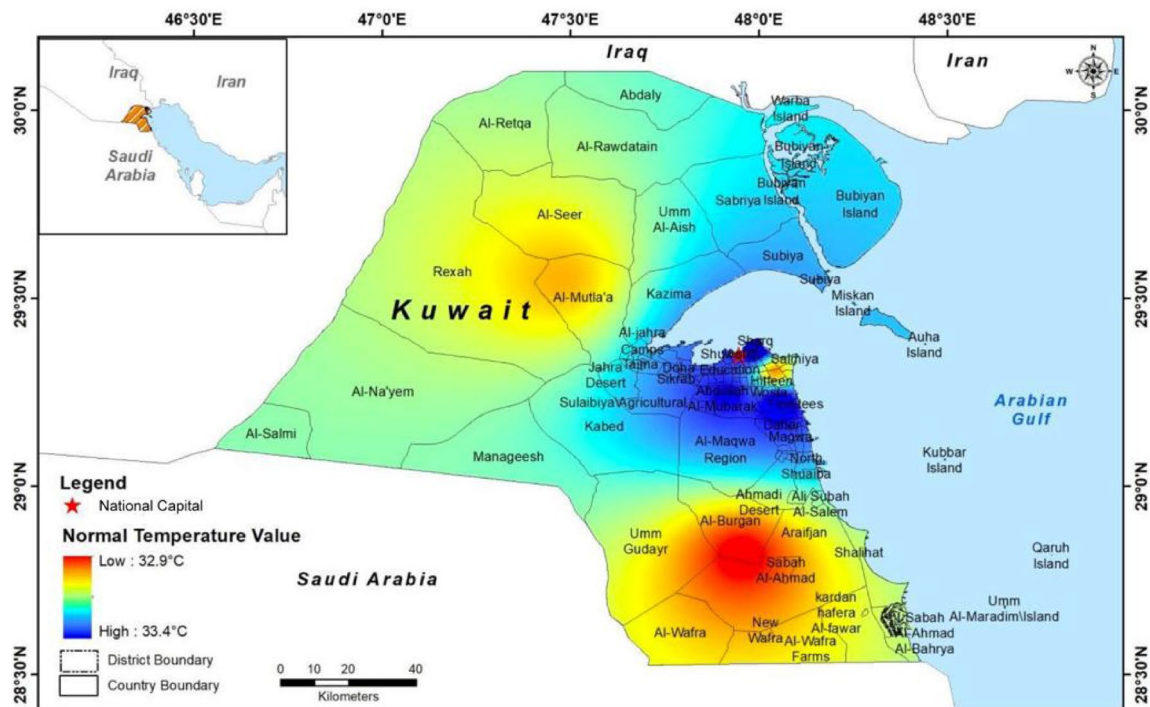
Fig. 8 Normal annual average maximum temperature distribution in Kuwait, 1981–2018. *Source* Kuwait Institute for Scientific Research (KISR)

Long-term seasonal rainfall data (October to May) for 38 years (1981–2018) were used for drought hazard mapping. The spatial rainfall distribution map (38-year average total rainfall for the rainy season) is shown in Fig. 7. The map shows that the northwestern part of Kuwait receives the highest average total rainfall (about 116.4 mm). In contrast, the southern part receives the lowest average total rainfall (about 88.0 mm).

The standardized precipitation index (SPI) is the most commonly used indicator for detecting and characterizing drought and is relatively easy to use (Erian et al. 2010). The standardized temperature index (STI) represents the probability of the occurrence of temperature. The STI is closely related to the SPI, as described by McKee et al. (1993). The SPI and STI indices provide valuable tools for drought hazard assessment (Li et al. 2021). Positive and negative STI values indicate temperatures above and below the median temperature of the long-term period, respectively. The STI and SPI indices were calculated for the period 1981–2018. The spatial distribution patterns of the normal annual average maximum temperature (that is, normal hot conditions) across Kuwait are shown in Fig. 8. The normal yearly average temperature across Kuwait is relatively similar (32.9–33.4 °C). Similar results were recorded using the SPI in other arid regions (Ali et al. 2017).

The SPI values were computed for 16 weather stations. It was assumed that the rainfall at a given weather station was independent of the rainfall in the surrounding stations.

Drought events based on the SPI values were computed using the historical rainfall data to generate the different drought return period (RP) maps. The inverse distance weight (IDW) spatial interpolation using ArcGIS 10.2 was used to interpolate SPI values across Kuwait. Drought hazard maps for 5-, 10-, 19-, and 38 year return periods were generated (Fig. 9). All districts within Kuwait are susceptible to minor drought at least once in a 5 year RP. In a 10 year RP, severe drought is expected in Kuwait City and north of Kuwait, and moderate drought is expected in the south of Kuwait. In contrast, severe drought is expected in all districts at least once in a 19 year period. In a 38 year RP, extreme drought is expected in Kuwait City and north and west of Kuwait, while severe drought is expected in the south of Kuwait. Drought provokes great concern across the Arab region (Sherif et al. 2014; Tomaszkiewicz 2021).

3.4 Air Pollution

Air quality over the AP, including Kuwait, has received significant attention during the past two decades due to unprecedented anthropogenic pollution (Farahat 2016; Alahmad et al. 2021). The annual mean levels of $PM_{2.5}$, PM_{10}, and NO_2 were shown to be significantly higher than both the World Health Organization (WHO) and Kuwait air quality limits (Al-Hemoud, Gasana et al. 2021). Air pollution was evaluated in compliance with air quality standards, and air pollution hazard maps were created using the United States
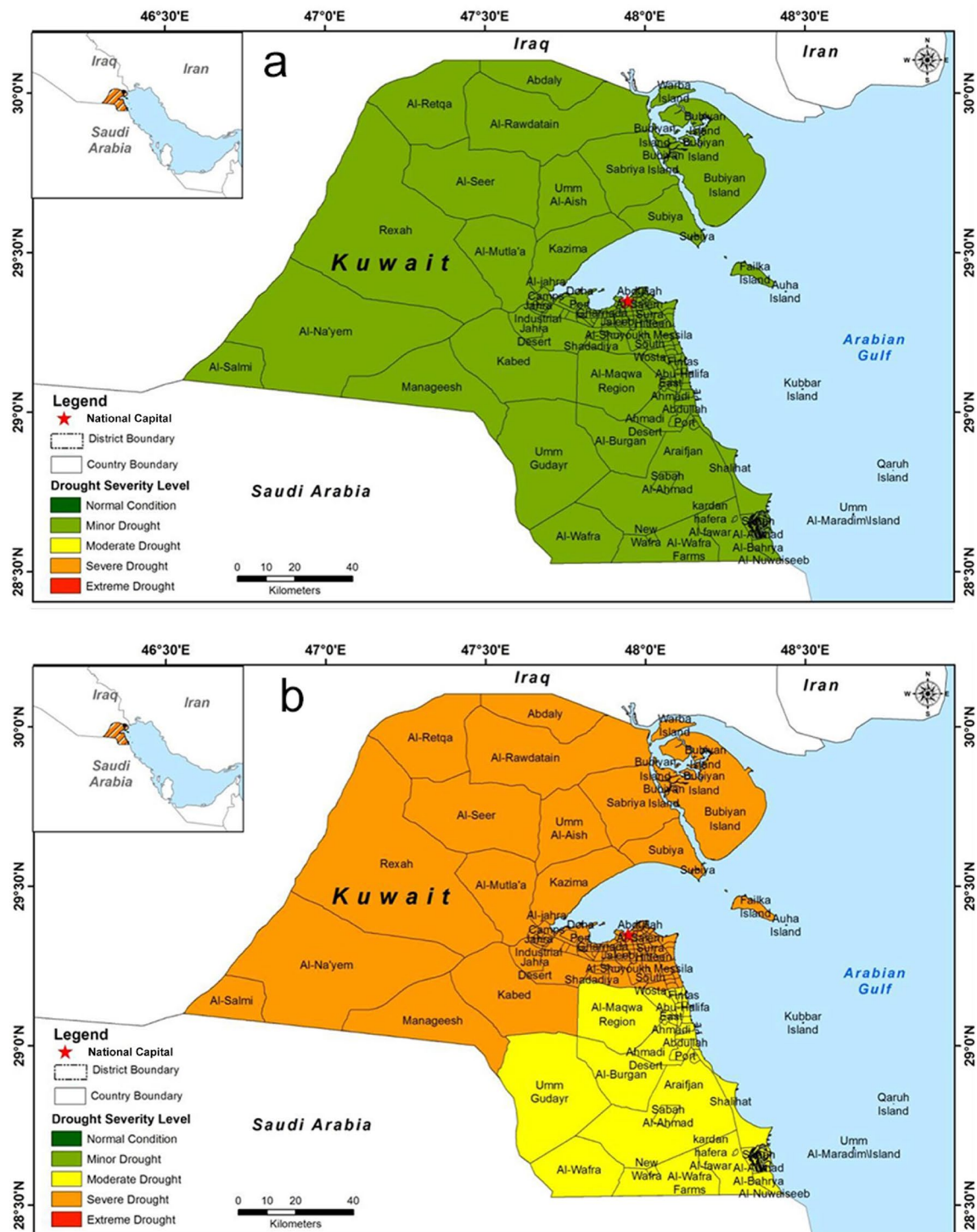
Fig. 9 Drought hazard maps for Kuwait for different return periods based on rainy season total rainfall data in 1981–2018: **a** 5 year; **b** 10 year; **c** 19 year; and **d** 38 year. *Source* Kuwait Institute for Scientific Research (KISR)

Environmental Protection Agency (US EPA) air quality index (AQI) (EPA 2018). Data for real-time hourly concentrations of PM_{10}, NO_2, and O_3 were gathered from 15 monitoring stations in Kuwait for four years (2014−2017).

The results show that the 4 year average PM_{10} concentration was 167.5 μg/m^3, which is 10 times greater than the WHO air quality guideline (15 μg/m^3) (WHO 2021). The 4 year average NO_2 concentration (35 ppb) exceeded both
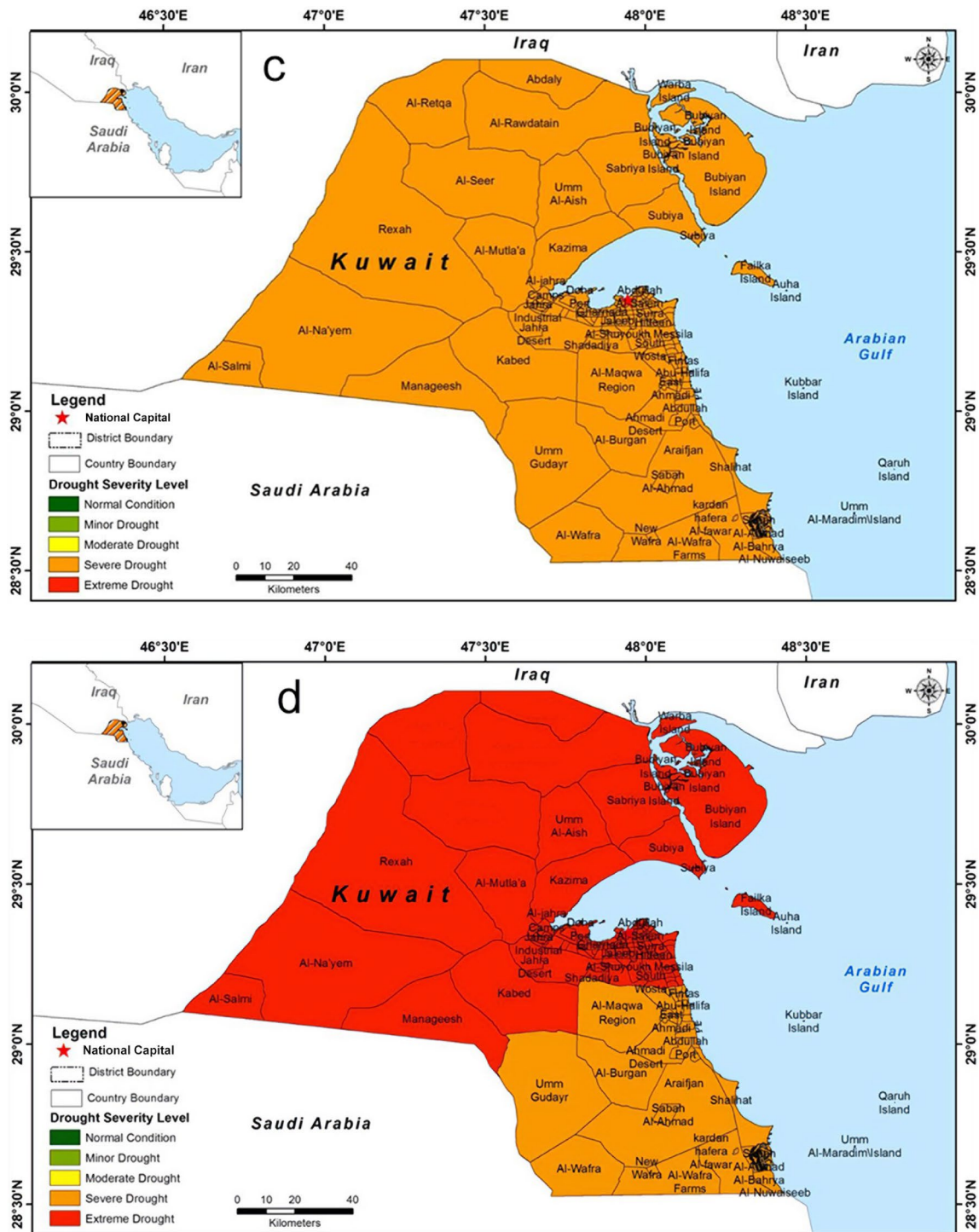
Fig. 9 (continued)

the WHO (5 ppb) and Kuwait limits (21 ppb), while the 8 h mean O_3 concentration (38 ppb) was significantly lower than Kuwait's 99th percentile of maximum concentration (70 ppb) and the 8 h mean of the WHO level (50 ppb).

The air pollution hazard maps are shown in Fig. 10. The figure shows that Al-Shuaiba had a good AQI of PM_{10}, while

Al-Shuwaikh had the poorest AQI. Poor AQI of PM_{10} in Al-Shuwaikh district may be associated with high traffic volume and many industrial workshops in the area (Al-Hemoud, Al-Khayat et al. 2021). As for NO_2, the poorest AQI is recorded at Road 50 station, which is located en route to the Kuwait International Airport, where traffic and heavy-duty
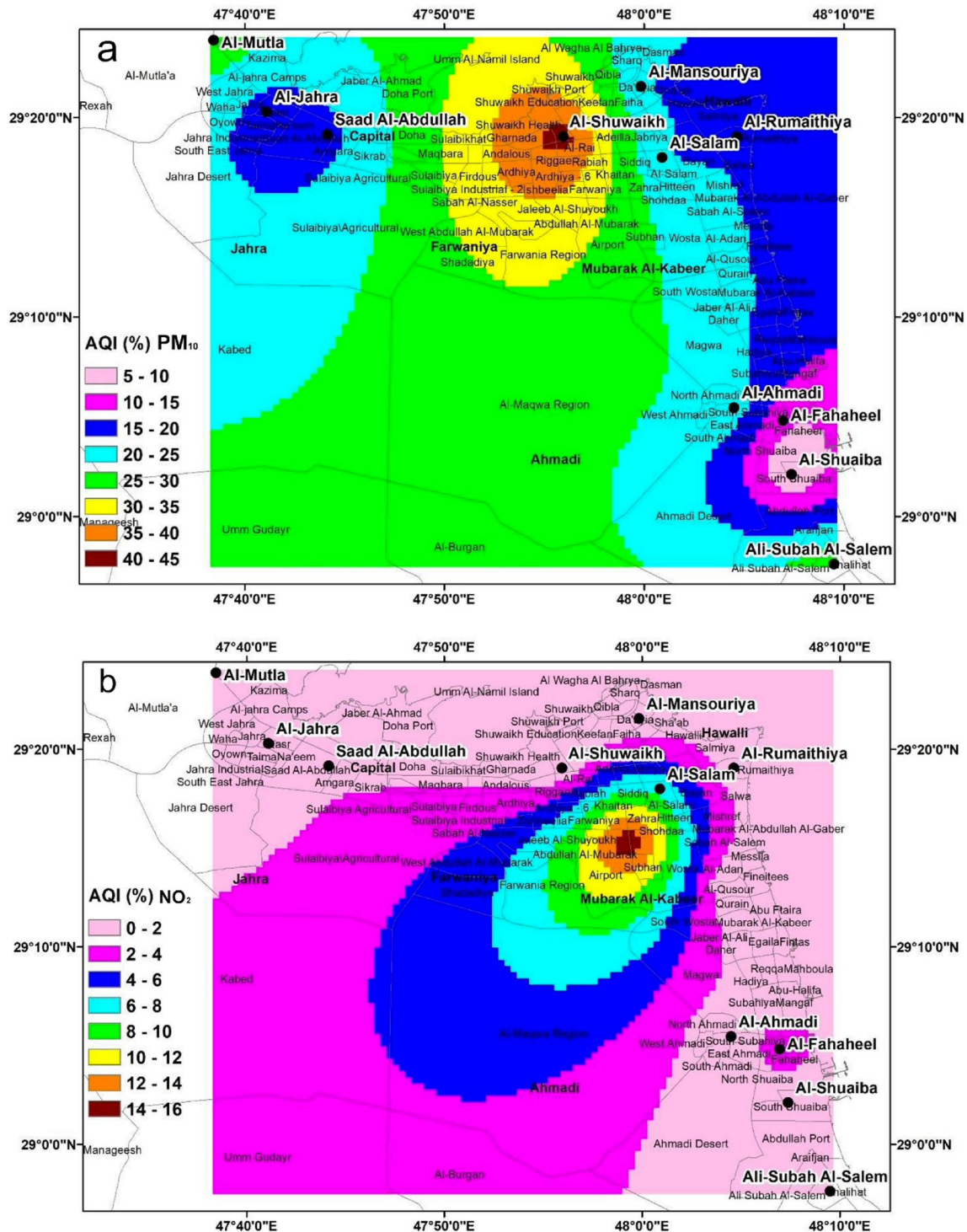
Fig. 10 Air pollution hazard maps for Kuwait based on 2014–2017 data: **a** PM$_{10}$; **b** NO$_2$; and **c** O$_3$. *Source* Kuwait Institute for Scientific Research (KISR).

diesel-engine vehicles are an ongoing presence (Al-Hemoud, Gasana et al. 2021). The AQI of O$_3$ is generally good for all stations except for Al-Fahaheel. It is well known that O$_3$ is scavenged in the presence of high NOx (Kroll et al. 2020).

3.5 Oil Spills

Oil spills are widespread in Kuwait because of oil drilling exploration, refineries, and export. Satellite remote sensing
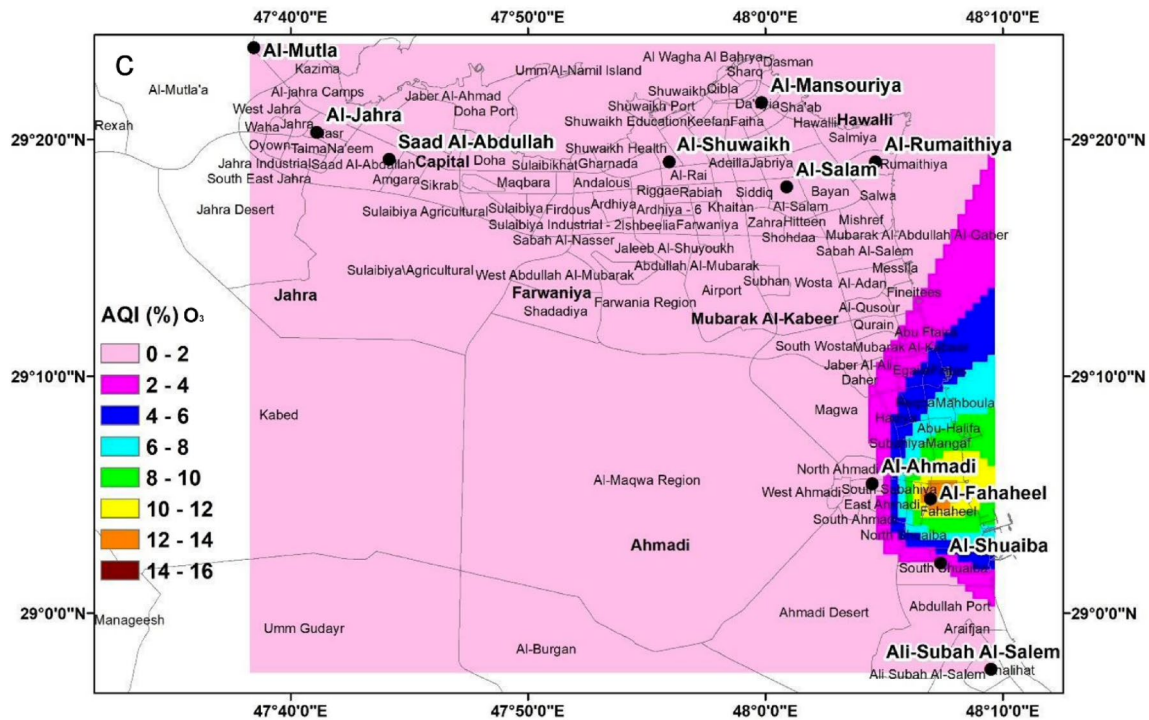
Fig. 10 (continued)

tools for oil spill detection are commonly used and operate in the visible, infrared, and thermal infrared bands (Fingas and Brown 2018). The contrast between oil and water enables much of the electromagnetic spectrum to detect oil spills. Space-borne Synthetic Aperture Radar (SAR) has proven useful in oil spill detection and monitoring (Nunziata et al. 2018; Naz et al. 2021). Comprehensive coverage provided by SAR-equipped satellites such as European Envisat creates an excellent opportunity to develop operational oil spill applications. We applied GIS and SAR imagery for oil spill hazard mapping. The SAR systems rely on the detection variation of the sea surface roughness. Oil films can be detected as dark patches relative to the surrounding water as they dampen the wind generated by short surface waves.

In this study, we mapped Kuwait's offshore and onshore oil spills. We used Sentinel-1 imagery to detect offshore deep-water horizon oil spills (Fig. 11). The downloaded images were processed through the SNAP tool to classify oil and water and delineate and map the extent of the oil spills. A total of 24 Sentinel-1 oil spill images were identified for offshore oil spill mapping (19 images in 2018 and 5 images in 2017). Besides offshore oil spills, eight onshore oil spills were identified (4 images in 2010 and 4 images in 2017). Landsat-7 enhanced thematic mapper plus (ETM+), Landsat-8 operational land imager (OLI), and multi-spectral instrument (MSI) were used to delineate onshore oil spills.

The offshore oil spill hazard map for Kuwait is shown in Fig. 12. Most offshore oil spill events have occurred in the southeast of Kuwait because of the oil tankers' travel pathways. Several seaports are located in this region, including the three main oil terminals (Mina Al-Ahmadi, Mina Abdullah, and Mina Al-Shuaiba). The offshore oil spills were observed around three islands (Qaruh, Bubiyan, and Failaka). The offshore oil spill extents vary from 3 to 750 km^2, and most spills occurred within 100–150 km from Kuwait City. The volume loss ranged between 3358 and 648,228 liters for the different offshore oil spill events. The onshore oil spills were mostly identified inside two major oil fields (Burgan and Al-Rawdatain). It was difficult to calculate the volume loss of onshore oil spills for various reasons, including absorption of oil into the soil, oil evaporation, and spilled oil covered by sand encroachment.

4 Discussion

In the present study, the hazard mapping profiles the main hazards that affect Kuwait. The Sendai Framework Data Readiness Review Report of Kuwait[1] notes that Kuwait lacks a country-level database for collecting disaster losses. It also

---

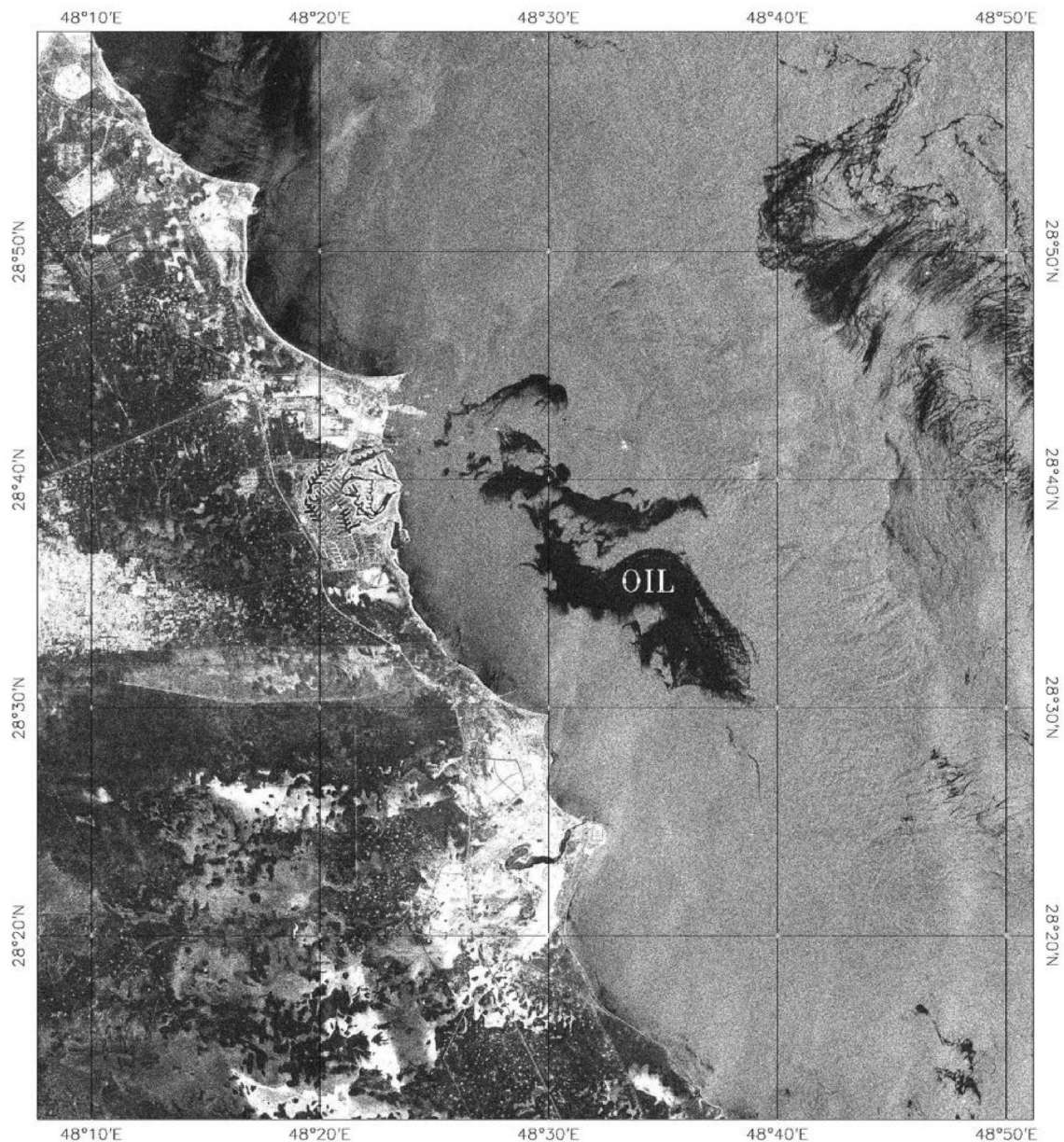[1] https://www.preventionweb.net/files/53141_kuwaitkwt.pdf

Fig. 11 Sentinel-1 imagery with deep-water horizon offshore oil spill in Kuwait on 30 June 2018. *Source* Kuwait Institute for Scientific Research (KISR).

notes that hazard-wise important information required for vulnerability and risk assessment is not presently captured by the current institutional mechanism. The report also notes that historically the State of Kuwait has not been severely impacted by highly catastrophic disaster events.

Kuwait is regularly affected by environmental and climatic hazards, including droughts, sand and dust storms (and associated sand encroachment), flash floods, and technological hazards such as oil spills and air pollution, gas/vapor leaks, and other flares and emissions that have become an increasingly growing concern as the economy of Kuwait

continues to thrive. To safeguard the country's already vulnerable population, addressing these environmental, climatic, and technological challenges is critical for Kuwait's economic competitiveness and sustainable development. This assessment will contribute to the creation of an enabling environment for demand-driven disaster risk management strategies. Additionally, hazard information generated through this process will be integrated into the broader Gulf Cooperative Countries' efforts for hazard and risk management. Currently, the Kuwait Institute for Scientific Research (KISR) acts as the centralized agency for the identification
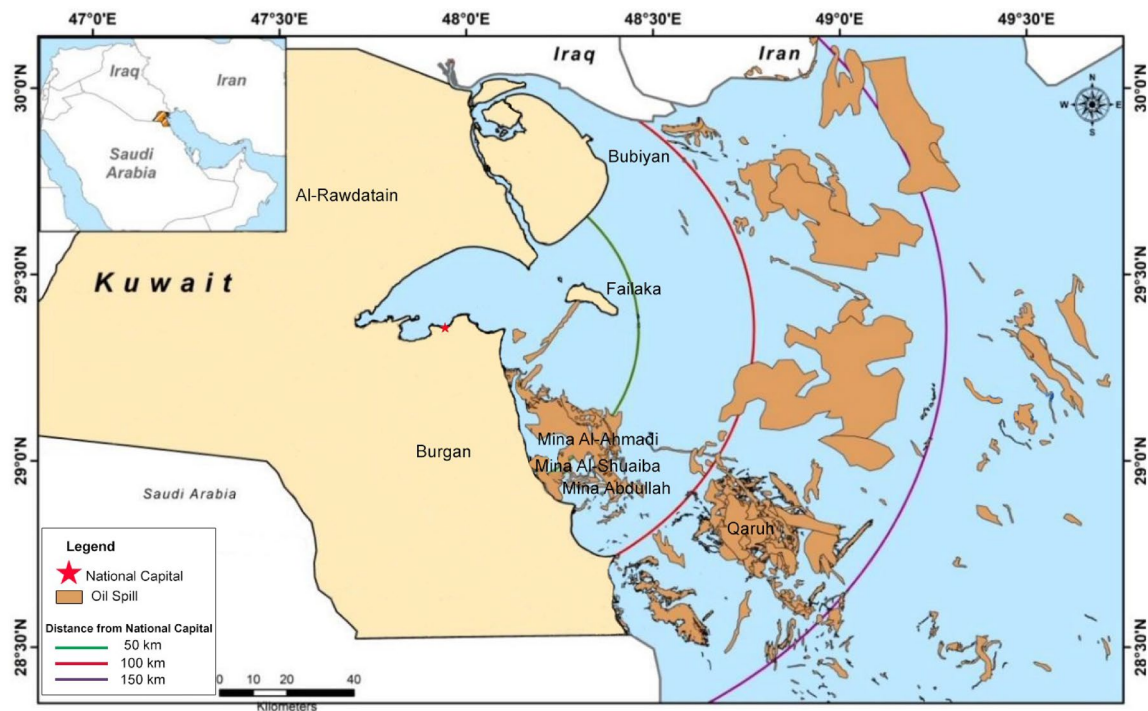
Fig. 12 Offshore oil spill hazard map for Kuwait based on 2010, 2017, and 2018 data. *Source* Kuwait Institute for Scientific Research (KISR)

of threats and mobilizing responses to mitigate and avert impacts of both natural and anthropogenic hazards. With the change in the global discourse towards disaster risk management, Kuwait recognizes the need for a proactive approach towards disaster and climate risk management. It is revamping its disaster risk management system.

The main objective of this study was to develop a macro-hazard assessment for the State of Kuwait, with a specific focus on Kuwait City, as a precursor for comprehensive disaster risk assessment, covering the hazards of surface water flooding, dust storms and sand encroachment, drought, air pollution, and oil spills.

The hazard maps are presented in terms of: (1) Digital spatial layers that describe the frequency and severity of sand and dust storms and associated sand encroachments, surface water flooding (flash floods), and droughts, and their interdependence where appropriate; (2) Digital spatial layers that describe probabilistic events for three air pollutants (PM_{10}, NO_2, O_3); and (3) Digital spatial layers that describe hazard areas of oil spills, accident based and natural, both onshore and offshore.

All the hazard distributions are delivered in GIS. These could be used in a variety of applications in planning, disaster mitigation, and so on. From simple overlay of hazard maps with various exposure elements, it is possible to evaluate whether a particular exposure element is vulnerable to a specific hazard. For example, by overlaying a school location layer over a 100 year return period flood hazard layer,

it is easy for a disaster manager to see which schools will be available for flood shelters and which may not. There is a requirement for risk assessment for the studied hazards for Kuwait. Therefore, for the assessment of risk from these hazards, both exposure and vulnerability must be quantified.

5 Conclusion

Hazards are generally studied in isolation but there is a great need to assess hazards holistically. The main goal of this study was to develop nationwide hazard maps for Kuwait. The motivation was the nonexistence of hazard assessment and hazard prioritization for Kuwait. This study assessed the hazards of most concern and generated hazard maps for "high-priority" hazards. Hazard identification and prioritization were conducted quantitatively (hazard data analysis) and qualitatively (participatory approach through questionnaires and governmental/institutional expert discussions). Geospatial techniques using remote sensing and GIS were utilized for hazard mapping. Out of the 25 identified hazards, nine were considered significant, of which five were selected as "high-priority" hazards. Hazard mapping identified vulnerable areas: (1) Kuwait City and suburban areas, coastal areas, north (Abdaly), and south (Sabah Al-Ahmad and Wafra) are considered flood-prone areas; (2) high/very high dust storm and sand encroachment hot spots are present in the west and south of Kuwait; (3) severe drought was

delineated in the south and extreme drought in the central, west, and north of Kuwait in a 10 year and 38 year RP; (4) high air pollution zones were identified around industrial and high-traffic areas; and (5) offshore oil spills were delineated around three main islands and three main oil terminals, while onshore oil spills were delineated inside Burgan and Al-Rawdatain oil fields. Using individual maps to convey information on each hazard can provide insightful information to decision makers and allows for ease of data editing, integration, and analysis. The generated hazard maps are vital visualization tools for disaster risk management.

References

Abdullah, W., A. Alzaza, R. Misak, and M. Amjad. 2021. Development of sustainable solutions to sand encroachment on roads in Kuwait using numerical modeling. *Journal of Engineering Research* 9(2): 43–59.

Ahmed, B., and I. Kelman. 2018. Measuring community vulnerability to environmental hazards: a method for combining quantitative and qualitative data. *Natural Hazards Review* 19(3): Article 04018008.

Al-Dousari, A.M., and J. Al-Awadhi. 2012. Dust fallout in northern Kuwait, major sources and characteristics. *Kuwait Journal of Science* 39(2A): 171–187.

Al-Hemoud, A., A. Al-Dousari, H. Al-Dashti, P. Petrov, A. Al-Saleh, S. Al-Khafaji, W. Behbehani, J. Li, and P. Koutrakis. 2020. Sand and dust storm trajectories from Iraq Mesopotamian flood plain to Kuwait. *Science of the Total Environment* 710: Article 136291.

Al-Hemoud, A., A. Al-Dousari, R. Misak, M. Al-Sudairawi, A. Naseeb, H. Al-Dashti, and N. Al-Dousari. 2019. Economic impact and risk assessment of sand and dust storms (SDS) on the oil and gas industry in Kuwait. *Sustainability* 11: Article 200.

Al-Hemoud, A., A. Al-Khayat, H. Al-Dashti, J. Li, B. Alahmad, and P. Koutrakis. 2021. PM2.5 and PM10 during COVID-19 lockdown in Kuwait: Mixed effect of dust and meteorological covariates. *Environmental Challenges* 5: Article 100215.

Al-Hemoud, A., J. Gasana, A. Alajeel, E. Alhamoud, A. Al-Shatti, and A. Al-Khayat. 2021. Ambient exposure of O3 and NO2 and associated health risk in Kuwait. *Environmental Science Pollution Research* 28: 14917–14926.

Alahmad, B., A. Al-Hemoud, C.M. Kang, F. Almarri, V. Kommula, J.M. Wolfson, A.S. Bernstein, E. Garshick, et al. 2021. A two-year assessment of particulate air pollution and sources in Kuwait. *Environmental Pollution* 282: Article 117016.

Alahmad, B., L.P. Tomasso, A. Al-Hemoud, P. James, and P. Koutrakis. 2020. Spatial distribution of land surface temperatures in Kuwait: Urban heat and cool islands. *International Journal of Environmental Research and Public Health* 17(9): Article 2993.

Ali, Z., I. Hussain, M. Faisal, H.M. Nazir, M. Abd-el Moemen, T. Hussain, and S. Shamsuddin. 2017. A novel multi-scalar drought index for monitoring drought: the standardized precipitation temperature index. *Water Resources Management* 31(3–4): 4957–4969.

Allen, T.R., T. Crawford, B. Montz, J. Whitehead, S. Lovelace, A.D. Hanks, A.R. Christensen, and G.D. Kearney. 2019. Linking water infrastructure, public health, and sea level rise: integrated assessment of flood resilience in coastal cities. *Public Works Management Policy* 24(72): 110–139.

Anderson-Berry, L.J. 2003. Community vulnerability to tropical cyclones: Cairns, 1996–2000. *Natural Hazards* 30(2): 209–232.

Antzoulatos, G., I.O. Kouloglou, M. Bakratsas, A. Moumtzidou, I. Gialampoukidis, A. Karakostas, F. Lombardo, R. Fiorin, et al. 2022. Flood hazard and risk mapping by applying an explainable machine learning framework using satellite imagery and GIS data. *Sustainability* 14: Article 3251.

Asim, M., A. Mekkodathil, B. Sathian, R. Elayedath, R. Kumar, P. Simkhada, E. Van Teijlingen. 2019. Post-traumatic stress disorder among the flood affected population in Indian subcontinent. *Nepal Journal of Epidemiology* 9: Article 755.

Athimon, E., and M. Maanan. 2018. Vulnerability, resilience and adaptation of societies during major extreme storms during the little ice age. *Climate of the Past* 14(10): 1487–1497.

Bae, S., S.H. Lee, S.H. Yoo, and T. Kim. 2018. Analysis of drought intensity and trends using the modified SPEI in South Korea from 1981 to 2010. *Water* 10: Articel 327.

Bang, H.N. 2022. A concise appraisal of Cameroon's hazard risk profile: multi-hazard inventories, causes, consequences and implications for disaster management. *GeoHazards* 3(1): 55–87.

Bathrellos, G.D., H.D. Skilodimou, K. Chousianitis, A.M. Youssef, and B. Pradhan. 2017. Suitability estimation for urban development using multi-hazard assessment map. *Science of the Total Environment* 575: 119–134.

Bird, D.K. 2009. The use of questionnaires for acquiring information on public perception of natural hazards and risk mitigation—A review of current knowledge and practice. *Natural Hazards and Earth System Sciences* 9(4): 1307–1325.

Brilly, M., and M. Polic. 2005. Public perception of flood risks, flood forecasting and mitigation. *Natural Hazards and Earth System Sciences* 5(3): 345–355.

Chiang, F., O. Mazdiyasni, and A. AghaKouchak. 2021. Evidence of anthropogenic impacts on global drought frequency, duration, and intensity. *Nature Communications* 12(1): 1–10.

Chouhan, S., and M. Mukherjee. 2022. Design and testing of a multi-hazard risk rapid assessment questionnaire for hill communities in the Indian Himalayan Region. Natural Hazards and Earth System Sciences Discussions. https://doi.org/10.5194/nhess-2022-91.

Clive, M.A.T., J.M. Lindsay, G.S. Leonard, C. Lutteroth, A. Bostrom, and P. Corballis. 2021. Volcanic hazard map visualisation affects

cognition and crisis decision-making. *International Journal of Disaster Risk Reduction* 55: Article 102102.

Cook, B.I., J.S. Mankin, and K.J. Anchukaitis. 2018. Climate change and drought: From past to future. *Current Climate Change Reports* 4: 164–179.

Dabanli, I. 2018. Drought risk assessment by using drought hazard and vulnerability indexes. Natural Hazards and Earth System Sciences Discussions. https://doi.org/10.5194/nhess-2018-129.

EPA (Environmental Protection Agency). 2018. Technical assistance document for the reporting of daily air quality—The air quality index (AQI). Office of air quality planning and standards, Air quality assessment division, Research Triangle Park, NC, USA.

Erian, E., B. Katlan, and O. Babah. 2010. *Drought vulnerability in the Arab region: global assessment report on disaster risk reduction*. Geneva: United Nations International Strategy for Disaster Reduction.

Eriksen, S.H., and P.M. Kelly. 2007. Developing credible vulnerability indicators for climate adaptation policy assessment. *Mitigation Adaptation Strategies for Global Change* 12(4): 495–524.

Farahat, A. 2016. Air pollution in the Arabian Peninsula (Saudi Arabia, the United Arab Emirates, Kuwait, Qatar, Bahrain, and Oman): Causes, effects, and aerosol categorization. *Arabian Journal of Geosciences* 9: Article 196.

Feng, B., J. Wang, Y. Zhang, B. Hall, and C. Zeng. 2020. Urban flood hazard mapping using a hydraulic–GIS combined model. *Natural Hazards* 100(3): 1089–1104.

Fingas, M., and C.E. Brown. 2018. A review of oil spill remote sensing. *Sensors* 18(1): Article 91.

Francis, D., J.P. Chaboureau, N. Nelli, J. Cuesta, N. Alshamsi, M. Temimi, O. Pauluis, and L. Xue. 2021. Summertime dust storms over the Arabian Peninsula and impacts on radiation, circulation, cloud development and rain. *Atmospheric Research* 250: Article 105364.

Gómez, D., P. Salvador, J. Sanz, C. Casanova, and J.L. Casanova. 2018. Detecting areas vulnerable to sand encroachment using remote sensing and GIS techniques in Nouakchott, Mauritania. *Remote Sensing* 10: Article 1541.

Grimaldi, S., A. Petroselli, E. Arcangeletti, and F. Nardi. 2013. Flood mapping in ungauged basins using fully continuous hydrologic-hydraulic modeling. *Journal of Hydrology* 487: 39–47.

Hamdan, A.N.A., S. Almuktar, and M. Scholz. 2021. Rainfall-runoff modeling using the HEC-HMS model for the Al-Adhaim River catchment, northern Iraq. *Hydrology* 8: Article 58.

Haynes, K., J. Barclay, and N. Pidgeon. 2008. Whose reality counts? Factors affecting the perception of volcanic risk. *Journal of Volcanology Geothermal Research* 172(3–4): 259–272.

Hermida, L., A. Merino, J. Sánchez, S. Fernández-González, E. García-Ortega, and L. López. 2018. Characterization of synoptic patterns causing dust outbreaks that affect the Arabian Peninsula. *Atmospheric Research* 199(4): 29–39.

Kalantari, Z., C.S.S. Ferreira, S. Keesstra, and G. Destouni. 2018. Nature-based solutions for flood-drought risk mitigation in vulnerable urbanizing parts of East-Africa. *Current Opinion in Environmental Science Health* 5: 73–78.

Kappes, M.S., M. Papathoma-Koehle, and M. Keiler. 2012. Assessing physical vulnerability for multi-hazards using an indicator-based methodology. *Applied Geography* 32(2): 577–590.

Kienberger, S., S. Lang, and P. Zeil. 2009. Spatial vulnerability units—expert-based spatial modelling of socio-economic vulnerability in the Salzach catchment, Austria. *Natural Hazards and Earth System Sciences* 9(3): 767–778.

Kroll, J.H., C.L. Heald, C.D. Cappa, D.K. Farmer, J.L. Fry, J.G. Murphy, and A.L. Steiner. 2020. The complex chemical effects of COVID-19 shutdowns on air quality. *Nature Chemistry* 12(9): 777–779.

Lamichhane, N., and S. Sharma. 2018. Effect of input data in hydraulic modeling for flood warning systems. *Hydrological Sciences Journal* 63(6): 938–956.

Li, J., E. Garshick, A. Al-Hemoud, S. Huang, and P. Koutrakis. 2020. Impacts of meteorology and vegetation on surface dust concentrations in Middle Eastern countries. *Science of the Total Environment* 712: Article 136597.

Li, J., Z. Wang, X. Wu, J. Zscheischler, S. Guo, and X. Chen. 2021. A standardized index for assessing sub-monthly compound dry and hot conditions with application in China. *Hydrology Earth System Sciences* 25: 1587–1601.

Lindell, M.K., and D.J. Whitney. 2000. Correlates of household seismic hazard adjustment adoption. *Risk Analysis* 20(1): 13–26.

Liu, K., M. Wang, Y. Cao, W. Zhu, and G. Yang. 2018. Susceptibility of existing and planned Chinese railway system subjected to rainfall-induced multi-hazards. *Transportation Research Part A: Policy Practice* 117: 214–226.

Mahendra, R., P. Mohanty, H. Bisoyi, T.S. Kumar, and S. Nayak. 2011. Assessment and management of coastal multi-hazard vulnerability along the Cuddalore–Villupuram, east coast of India using geospatial techniques. *Ocean Coastal Management* 54: 302–311.

McKee, T.B., N.J. Doesken, and J. Kleist. 1993. The relationship of drought frequency and duration to time scales. In *Proceedings of the 8th Conference on Applied Climatology*, 17–22 January 1993, Boston, USA, 179–183.

Mehrabi, A. 2020. Detecting areas vulnerable to sand encroachment using remote sensing and GIS techniques; Case study: Rigan, Fahraj and Narmashir Counties, Kerman Province. *Journal of Natural Environmental Hazards* 9: 47–62.

Merlone, A., H. Al-Dashti, N. Faisal, R.S. Cerveny, S. AlSarmi, P. Bessemoulin, M. Brunet, and F. Driouech et al. 2019. Temperature extreme records: World meteorological organization metrological and meteorological evaluation of the 540 °C observations in Mitribah, Kuwait and Turbat, Pakistan in 2016/2017. *International Journal of Climatology* 39(13): 5154–5169.

Michikawa, T., S. Yamazaki, A. Shimizu, H. Nitta, K. Kato, Y. Nishiwaki, and S. Morokuma. 2020. Exposure to Asian dust within a few days of delivery is associated with placental abruption in Japan: a case-crossover study. *BJOG: An International Journal of Obstetrics Gynaecology* 127(3): 335–342.

Miles, S., and D. Keefer. 2009. Toward a comprehensive areal model of earthquake-induced landslides. *Natural Hazards Review* 10(1): 19–28.

Mokhtar, E.S., B. Pradhan, A.H. Ghazali, and H.Z.M. Shafri. 2018. Assessing flood inundation mapping through estimated discharge using GIS and HEC-RAS model. *Arabian Journal of Geosciences* 11: Article 682.

Mun, Y.S., W.H. Nam, M.G. Jeon, N.K. Bang, and T. Kim. 2020. Assessment of vulnerability to drought disaster in agricultural reservoirs in South Korea. *Atmosphere* 11: Article 1244.

Nachappa, T.G., O. Ghorbanzadeh, K. Gholamnia, and T. Blaschke. 2020. Multi-hazard exposure mapping using machine learning for the State of Salzburg, Austria. *Remote Sensing* 12: Article 2757.

Nam, W.H., M.J. Hayes, M.D. Svoboda, T. Tadesse, and D.A. Wilhite. 2015. Drought hazard assessment in the context of climate change for South Korea. *Agricultural Water Management* 160: 106–117.

Nasrollahi, M., H. Khosravi, A. Moghaddamnia, A. Malekian, and S. Shahid. 2018. Assessment of drought risk index using drought hazard and vulnerability indices. *Arabian Journal of Geosciences* 11: Article 606.

Naz, S., M.F. Iqbal, I. Mahmood, and M. Allam. 2021. Marine oil spill detection using Synthetic Aperture Radar over Indian Ocean. *Marine Pollution Bulletin* 162: Article 111921.

Newarab. 2018. Kuwait flood damages estimated at over $300 million. https://www.alaraby.co.uk/english/news/2018/11/12/kuwait-flood-damages-estimated-at-over-300-million. Accessed 30 Jan 2023.

Nguyen, T.T., J. Bonetti, K. Rogers, and C.D. Woodroffe. 2016. Indicator-based assessment of climate-change impacts on coasts: a review of concepts, methodological approaches and vulnerability indices. *Ocean Coastal Management* 123: 18–43.

Nones, M. 2017. Flood hazard maps in the European context. *Water International* 42(3): 324–332.

Ntajal, J., B.L. Lamptey, I.B. Mahamadou, and B.K. Nyarko. 2017. Flood disaster risk mapping in the lower Mono river basin in Togo, West Africa. *International Journal of Disaster Risk Reduction* 23: 93–103.

Nunziata, F., A. Buono, and M. Migliaccio. 2018. COSMO–SkyMed synthetic aperture radar data to observe the deepwater horizon oil spill. *Sustainability* 10: Article 3599.

Nyarko, B.K., B. Diekkrüger, N.C. Van De Giesen, and P.L. Vlek. 2015. Floodplain wetland mapping in the White Volta river basin of Ghana. *GIScience Remote Sensing* 52(3): 374–395.

Orimoloye, I.R., J.A. Belle, A.O. Olusola, E.T. Busayo, and O.O. Ololade. 2021. Spatial assessment of drought disasters, vulnerability, severity and water shortages: a potential drought disaster mitigation strategy. *Natural Hazards* 105(3): 2735–2754.

Pandey, R., and S. Jha. 2012. Climate vulnerability index-measure of climate change vulnerability to communities: a case of rural Lower Himalaya, India. *Mitigation Adaptation Strategies for Global Change* 17: 487–506.

Park, S., S.J. Kim, H. Yu, C.H. Lim, E. Park, J. Kim, and W.K. Lee. 2020. Developing an adaptive pathway to mitigate air pollution risk for vulnerable groups in South Korea. *Sustainability* 12: Article 1790.

Park, S.H., H.S. Jung, M.J. Lee, W.J. Lee, and M.J. Choi. 2019. Oil spill detection from PlanetScope satellite image: application to oil spill accident near Ras Al Zour area, Kuwait in August 2017. *Journal of Coastal Research* 90(sp1): 251–260.

Pourghasemi, H.R., A. Gayen, M. Panahi, F. Rezaie, and T. Blaschke. 2019. Multi-hazard probability assessment and mapping in Iran. *Science of the Total Environment* 692: 556–571.

Rolfe, M.I., S.W. Pit, J.W. McKenzie, J. Longman, V. Matthews, R. Bailie, and G.G. Morgan. 2020. Social vulnerability in a high-risk flood-affected rural region of NSW. *Australia. Natural Hazards* 101(3): 631–650.

Sajjad, M., Y. Li, Z. Tang, L. Cao, and X. Liu. 2018. Assessing hazard vulnerability, habitat conservation, and restoration for the enhancement of mainland China's coastal resilience. *Earth's Future* 6: 326–338.

Sarmah, T., S. Das, A. Narendr, and B.H. Aithal. 2020. Assessing human vulnerability to urban flood hazard using the analytic hierarchy process and geographic information system. *International Journal of Disaster Risk Reduction* 50: Article 101659.

Sathya, A., and S.G. Thampi. 2021. Flood inundation mapping of Cauvery River using HEC-RAS and GIS. *Advances in Civil Engineering* 83: 15–23.

Shah, A.A., J. Ye, M. Abid, J. Khan, and S.M. Amir. 2018. Flood hazards: household vulnerability and resilience in disaster-prone districts of Khyber Pakhtunkhwa province. *Pakistan. Natural Hazards* 93(1): 147–165.

Sherif, M., M. Almulla, A. Shetty, and R.K. Chowdhury. 2014. Analysis of rainfall, PMP and drought in the United Arab Emirates. *International Journal of Climatology* 34(4): 1318–1328.

Solana, M.C., and C.R. Kilburn. 2003. Public awareness of landslide hazards: the Barranco de Tirajana, Gran Canaria. *Spain. Geomorphology* 54(1–2): 39–48.

Song, J., Z. Chang, W. Li, Z. Feng, J. Wu, Q. Cao, and J. Liu. 2019. Resilience-vulnerability balance to urban flooding: a case study in a densely populated coastal city in China. *Cities* 95: Article 102381.

Spinoni, J., J.V. Vogt, G. Naumann, P. Barbosa, and A. Dosio. 2018. Will drought events become more frequent and severe in Europe?. *International Journal of Climatology* 38(4): 1718–1736.

Tahmid, M., S. Dey, and S.R. Syeda. 2020. Mapping human vulnerability and risk due to chemical accidents. *Journal of Loss Prevention in the Process Industries* 68: Article 104289.

Tamiru, H., and M.O. Dinka. 2021. Application of ANN and HEC-RAS model for flood inundation mapping in lower Baro Akobo River Basin, Ethiopia. *Journal of Hydrology: Regional Studies* 36: Article 100855.

Tilloy, A., B.D. Malamud, H. Winter, and A. Joly-Laugel. 2019. A review of quantification methodologies for multi-hazard interrelationships. *Earth-Science Reviews* 196: Article 102881.

Tomaszewski, B.M., E.A. Moore, K. Parnell, A.M. Leader, W.R. Armington, O. Aponte, L. Brooks, B.K. Herold, et al. 2020. Developing a geographic information capacity (GIC) profile for disaster risk management under United Nations framework commitments. *International Journal of Disaster Risk Reduction* 47: Article 101638.

Tomaszkiewicz, M.A. 2021. Future seasonal drought conditions over the CORDEX-MENA/Arab Domain. *Atmosphere* 12: Article 856.

UNDRR (United Nations Office for Disaster Risk Reduction). 2022. Terminology. Geneva: United Nations Office for Disaster Risk Reduction. www.undrr.org/terminology. Accessed 15 Aug 2022.

Urrutia-Pereira, M., L.V. Rizzo, P.L. Staffeld, H.J. Chong-Neto, G. Viegi, and D. Solé. 2021. Dust from the Sahara to the American Continent: health impacts: dust from Sahara. *Allergologia et Immunopathologia* 49: 187–194.

WHO (World Health Organization). 2021. WHO global air quality guidelines—Particulate matter ($PM_{2.5}$ and PM_{10}), ozone, nitrogen dioxide, sulfur dioxide and carbon monoxide. Geneva: World Health Organization.

Yadav, D.K., and A. Barve. 2017. Analysis of socioeconomic vulnerability for cyclone-affected communities in coastal Odisha, India. *International Journal of Disaster Risk Reduction* 22: 387–396.

Yassin, M., S. Almutairi, and A. Al-Hemoud. 2018. Dust storms backward trajectories' and source identification over Kuwait. *Atmospheric Research* 212: 158–171.